Bangladesh J. Bot. **54**(3): 875-883, 2025 (September) Special DOI: https://doi.org/10.3329/bjb.v54i30.85168

PREDICTION OF MAIZE CHLOROPHYLL NITROGEN CONTENT USING VISIBLE AND NEAR-INFRARED SPECTROSCOPY

HANQI GAO*, MIN KANG, YUXIANG ZHU, YONGGUI CHEN AND HONGCHAO LI

Henan College of Surveying and Mapping, Zhengzhou, 451464, China

Keywords: Maize, Chlorophyll content, Visible and Near-Infrared Spectroscopy, Machine learning

Abstract

Chlorophyll quantification in summer maize (*Zea mays* L.) leaves is the focus of this research, specifically at the jointing phenological stage. Based on field experiments and the correlation between canopy spectral characteristics and chlorophyll during typical growth stages, the spectral reflectance of corn leaf samples was determined using an ASD FieldSpec Pro spectrometer with a wavelength range of 350-2500 nm. Variations in spectral reflectance patterns were examined across different chlorophyll concentrations. The reflectance spectra underwent Savitzky-Golay 9-point smoothing, followed by preprocessing with MSC and SNV. Subsequently, first-derivative, second-derivative, and reciprocal logarithmic transformations were applied. PLSR was employed to establish optimal spectral estimation models for chlorophyll. The results provide a theoretical foundation and technical guidance for non-destructive crop growth monitoring and precision nitrogen management. Reflectance spectra processed with Savitzky-Golay 9-point smoothing combined with different transformations significantly improved the signal-to-noise ratio. Derivative transformations enhanced the correlation between spectral data and corn leaf chlorophyll content. Using highly correlated combination bands substantially improved model stability and predictive capability. For PLSR models, the optimal approach involved MSC processing of smoothed spectra followed by second-derivative transformation, achieving Rc^2=0.9799, RMSEC=3.3027, and SEC=3.3225. The prediction models developed using various analytical approaches exhibited robust consistency and precise performance, facilitating efficient chlorophyll level assessment in large-scale maize fields.

Introduction

As the principal photon-capturing biomolecule in corn, chlorophyll plays a critical role in modulating photosynthetic quantum yield and carbon assimilation dynamics. Its foliar concentration provides a biophysical signature correlating with nitrogen utilization efficiency ($R^2 \geq 0.91$) (Wang and Bai 2005), photosystem II operational integrity (Croft *et al.* 2020), and abiotic stress tolerance thresholds (Dong *et al.* 2008). Empirical evidence confirms that chlorophyll metrics can predict more than 87% of the variation in final kernel mass through carboxylation enzyme activation cascades (Silva *et al.* 2018). High chlorophyll density during reproductive development (BBCH 60-69) increases RuBisCO turnover by 22–38%, leading to significant improvements in canopy-level CO_2 fixation efficiency (Wang and Bai 2005). Hyperspectral diagnostics exploit chlorophyll's unique absorption minima at 550 ± 3 nm (chlorophyll-b peak) and 675-685nm (P680 reaction center band) for pre-symptomatic nutrient deficiency detection. This non-invasive monitoring capability enables dynamic precision nitrogen management (Cedric *et al.* 2016), positioning chlorophyll quantification as an indispensable component in sustainable intensification frameworks for this globally strategic cereal crop supporting 1.2 billion human populations and livestock systems (Li *et al.* 2024).

While conventional chlorophyll measurement techniques, while capable of achieving relatively accurate results, are often operationally intensive, time-consuming, and typically require

*Author for correspondence: <ghq0119@163.com>.

destructive sampling (Li *et al.* 2023). These limitations restrict their applicability for real-time, rapid, non-destructive, and large-scale monitoring needs. In contrast, hyperspectral remote sensing technology offers advantages such as high efficiency, cost-effectiveness, minimal sample requirements, non-invasiveness, and delivers comprehensive data acquisition (Berger *et al.* 2021). The theoretical basis for retrieving chlorophyll content using spectral technology lies in the distinct absorption spectral characteristics of chlorophyll molecules (Ustin *et al.* 2009). While demonstrating high reflectance in the near-infrared band (700–900 nm). By establishing quantitative relationship models between spectral parameters and chlorophyll content, non-destructive monitoring of chlorophyll levels can be achieved (Verrelst *et al.* 2015). This approach allows for the monitoring of crop growth and nutritional status without compromising plant structural integrity, demonstrating considerable potential in predicting chlorophyll content (Yao *et al.* 2021). While chlorophyll levels in individual plants reflect data at the specimen level, the chlorophyll content within the crop canopy serves as a critical focal point in remote sensing applications (Houborg *et al.* 2015). Consequently, real-time monitoring of canopy leaf chlorophyll content holds significant value for remotely evaluating crop vigor, forecasting yield, and managing pest and disease interventions (Berger *et al.* 2018). Owing to the distinct molecular configuration of chlorophyll, electrons undergo energy level transitions upon absorbing light energy, resulting in spectral absorption peaks that are predominantly located within the visible light band (Porcar-Castell *et al.* 2014).

Employed near-infrared spectroscopy combined with standard normal variate (SNV) and detrending preprocessing methods to analyze leaves at the seedling stage. Their results demonstrated that within the spectral range of 3300–10000 cm^{-1}, a quantitative analysis model established using partial least squares regression (PLSR) achieved a coefficient of determination (R^2) of 0.989 and a root mean square error (RMSE) of 0.047, confirming the feasibility of rapidly detecting chlorophyll content in maize seedling leaves via near-infrared spectroscopy (Zhai and Li 2014). Sun *et al.* (2015) developed a 2-CCD multispectral imaging system capable of simultaneously capturing visible (blue, green, red) and near-infrared band images of maize canopies. By extracting the average grayscale values of each band and calculating eight vegetation indices—including the Ratio Vegetation Index (RVI) and Normalized Difference Vegetation Index (NDVI)—they constructed a multiple linear regression model for chlorophyll estimation. The study revealed negative correlations between the average grayscale values of visible light bands (R, G, B) and chlorophyll content (correlation coefficients ranging from –0.71 to –0.73), whereas NDVI showed a positive correlation with chlorophyll content. The model developed using multiple parameter combinations yielded a calibration set R^2 of 0.79 and a validation set R^2 of 0.71, providing an effective approach for non-destructive monitoring of chlorophyll in field maize canopies. Wang *et al.* (2023) systematically investigated hyperspectral inversion methods for estimating chlorophyll content and water content in maize leaves under drought stress. Using a hyperspectral camera, they collected images of seedling maize leaves subjected to varying degrees of drought stress, extracted average spectral data from the mesophyll region via image processing techniques, and compared the performance of different feature wavelength selection methods combined with machine learning regression models. Zhou and Chen (2025) explored the feasibility of integrating multi-source UAV remote sensing imagery with multiple machine learning methods to invert SPAD values in maize. Based on field experiments with different fertilization treatments, they acquired UAV multispectral and RGB images during the four-leaf and nine-leaf stages of maize growth. Using multi-scale analysis techniques, they fused the two types of imagery to generate integrated images that exhibit both high spatial resolution and multispectral characteristics.

Contemporary spectral quantification has undergone a paradigm shift from broadband detection to photon-level interactions. Third-generation hyperspectral imaging (HSI) systems now achieve <5 nm resolution, enabling picosecond-scale capture of energy transfer pathways in Photosystem II reaction centers through time-resolved fluorescence (Clark *et al.* 2022). Deep learning architectures like spectral Transformers utilize self-attention mechanisms to autonomously identify 17 chlorophyll-sensitive sub-bands within 450-750 nm, enhancing modeling accuracy by 23.8% versus conventional indices (Chen and Li 2024). Notably, laser-induced breakdown spectroscopy (LIBS)-Raman integration enables non-destructive in situ chlorophyll a/b ratio analysis, validating thylakoid membrane reorganization effects on spectral responses (<0.05 RMSE).

Spectral feature extraction is a core step in building high-precision chlorophyll retrieval models. Its objective is to condense the full-band spectral data into information that is highly sensitive to chlorophyll variation and resistant to interference. This technology has evolved significantly from parameterization designs relying on a priori knowledge to intelligent, data-driven mining, with various research teams making key contributions. Regarding "red edge" parameters, Miller *et al.* (1990) were among the first to systematically elaborate the intrinsic relationship between leaf chlorophyll content and the shift of the "Red Edge Position" within the red to near-infrared spectral region, observing a "red shift" of the REP with increasing chlorophyll concentration. Field studies by Filella and Peñuelas (1994) further established quantitative relationships between the REP displacement and the physiological stress status of crops, establishing it as a key indicator for vegetation health monitoring. In quantifying absorption features, Kokaly and Clark (1999) successfully introduced the continuum removal method, mature in geological remote sensing, into the retrieval of vegetation biochemical components. Their research approach, which involves constructing a spectral envelope and normalizing absorption features, effectively strips background noise, thereby enabling accurate quantification of characteristic parameters like the absorption depth and area of chlorophyll in the blue and red bands, significantly enhancing the feature's indicativeness for chlorophyll concentration.

In supervised linear feature compression, the Partial Least Squares Regression (PLSR) method established and promoted found widespread application in chemometrics (Wold *et al.* 2001). This method works by jointly projecting spectral variables and measured chlorophyll values into a new latent variable space, automatically finding spectral combinations that co-vary most with chlorophyll changes. Dorigo *et al.* (2007) noted in their review that for vegetation parameter retrieval, the effectiveness of feature extraction and the robustness of PLSR models were significantly superior to unsupervised methods like Principal Component Analysis. In the field of nonlinear and intelligent feature learning, Camps-Valls *et al.* (2006, 2011) conducted pioneering work by introducing kernel-based machine learning methods like Support Vector Regression and Gaussian Process Regression into biophysical parameter retrieval. These methods utilize kernel functions for nonlinear mapping, automatically learning complex relationships between chlorophyll and spectra in high-dimensional feature spaces. Recently, deep learning has enabled end-to-end feature learning. For instance, Yao *et al.* (2021) applied a one-dimensional Convolutional Neural Network (1D-CNN) to process hyperspectral curves. Their model can automatically learn hierarchical features from the original data, ranging from local absorption troughs to global spectral shapes, outperforming traditional models reliant on manually designed indices. The radiative transfer models developed by laid the theoretical foundation for this direction (Jacquemoud *et al.* 2009). Berger *et al.* (2018) detailed how to use such physical models to generate simulated spectral datasets covering various scenarios, which are then used to train machine learning models, ensuring that the extracted features are naturally physically constrained. Verrelst *et al.* (2013) further advanced this field with algorithms like "Gaussian Process Retrieval," successfully incorporating the uncertainties of physical models into a Bayesian learning framework. This achieves robust feature optimization and parameter inversion guided by physical mechanisms, greatly enhancing model transferability across different environments and crop species.

Multi-platform synergetic observation emerges as a key trend: Drone-mounted micro-HSI (μ-HSI) achieves cellular-scale imaging (0.2 μm/pixel), while satellite hyperspectral sensors demonstrate field-level prediction errors as low as 3.2 μg/cm² via 3D radiative transfer models incorporating leaf angle distribution (Kim *et al.* 2024). Quantum dot-enhanced spectral chips represent a breakthrough, leveraging surface plasmon resonance to boost red-edge shift detection sensitivity to 0.03 nm, enabling early nitrogen stress alerts 5-7 days pre-symptom. Current research evolves toward multimodal intelligent sensing: Integrating leaf thermal fields, spectral data, and environmental variables, dynamic coupling models in China's summer maize belt achieve unprecedented stability ($R^2 = 0.93 \pm 0.02$) across growth stages-significantly outperforming single-source systems (<0.82). These advances establish the photonic foundation for digital twin farmlands.

This study focuses on the chlorophyll content in leaves of summer maize during the jointing stage. Based on field experiments, we comprehensively integrate crop spectral characteristics, growth patterns, nutrient uptake dynamics, and biophysical parameter measurements with statistical analysis. By establishing correlations between canopy spectral features and key indicators (nitrogen status, biomass, and nitrogen uptake) across distinct growth stages, we develop stage-specific diagnostic models for nitrogen and biomass quantification. These models ultimately form the foundation for constructing spectral-based nitrogen application models.

Materials and Methods

This study selected typical farmland in Zhengzhou City, Henan Province as the research area, specifically located at 112°42′-114°14′E and 34°16′-34°58′N. The site is located on the southern bank of the middle-lower Yellow River, bordered by the Songshan Mountains to the west and the Huang-Huai Plain to the southeast. The terrain slopes from higher elevations in the southwest to lower areas in the northeast. The highest point is Shaoshi Peak in Dengfeng (1,512.4 m), while the lowest elevation is in Hansi Township, Zhongmu County (73 m), with the urban area averaging approximately 162 m above sea level. The warm-temperate continental monsoon climate (Köppen Dwa) delivers 14.4°C mean annual temperature with extreme monthly means: 0.2°C (Jan) and 27.3°C (Jul), confirming strong seasonality. Annual precipitation averages 640.9 mm, predominantly concentrated during summer (June-August accounting for >60% of the total). The frost-free period spans 220 days annually. Dominant soil types include Fluvo-aquic, Cinnamon, and Shajiang Black soils. The eastern plains feature deep, fertile soil layers optimal for intensive cultivation.

The trial was conducted annually with sowing in mid-June and harvesting in late September. Measurements were taken at six growth stages i.e., seedling, jointing, booting, tasseling, flowering, and milk-ripe. Seven nitrogen levels (0, 40, 80, 120, 160, 200, 240 kg N ha^{-1}) were applied in a 4:6 split ratio at seedling and booting stages. Pre-plant soil analyses included topsoil organic matter and total nitrogen. Manual plowing and harrowing with spades were performed before planting. Plot dimensions were 5×8 m² with three replicates per treatment.

Leaf spectral reflectance was acquired using an ASD FieldSpec Pro spectroradiometer (350-2500 nm range). Spectral parameters included: 350-1000 nm (1.4 nm sampling interval, 3 nm resolution) and 1001-2500 nm (2 nm sampling interval). Field spectroscopy measurements were consistently conducted under optimal atmospheric conditions (wind-free and clear skies) during the August 7, 2021 field campaign, and the measurement time was between 12:00 and 16:00. Spectral reflectance measurements were acquired from 15 randomly sampled canopy leaves representing distinct vertical positions within each experimental plot, and the spectral data of each plant were calibrated against a standard whiteboard. The canopy spectral reflectance for each sample was calculated as the mean of 10 spectral measurements per leaf, following the elimination of anomalous spectra.

Chlorophyll content in plant canopies was determined employing a portable CCM-200 meter (Opti-Sciences, USA), with 15 randomly selected leaves measured per experimental plot. To minimize the influence of outliers introduced during sample collection, processing, and analysis on subsequent modeling accuracy, the Mahalanobis distance method was employed to identify outliers in both soil properties and spectral data. This method is grounded in multivariate normal distribution theory, taking into account covariance, mean, and variance, thereby providing a comprehensive reflection of the overall variability among samples.

The averaged spectral curves were smoothed and denoised using the Savitzky–Golay 9-point convolution smoothing method to enhance the signal-to-noise ratio. Subsequently, first-order derivative, second-order derivative, and inverse logarithmic transformation of reflectance were applied to the smoothed curves to suppress background and baseline interference, thereby strengthening the correlation between spectral reflectance and soil organic carbon content. In addition to analyzing the original leaf spectral reflectance, three derivative transformations were performed to identify chlorophyll-sensitive regions under different transformation forms. The first-order derivative helps emphasize target reflectance while suppressing linear or near-linear background effects. The second-order derivative mitigates the influence of quadratic noise and high-frequency interference among components, facilitating the quantitative extraction of soil factors. The logarithmic transformation not only enhances spectral differences in the visible region but also reduces multiplicative effects caused by varying illumination conditions. Furthermore, multiplicative scatter correction and standard normal variate transformation were applied to effectively correct baseline shifts caused by sample scattering. By performing regression analysis between measured spectra and a reference spectrum, slope and intercept corrections were implemented, thereby reducing the effects of surface scattering and optical path variations.

The dataset was randomly split into a modeling set (70%) and a validation set (30%), used respectively for constructing the chlorophyll content prediction model and evaluating model performance. Correlation analysis was conducted using SPSS 17.0, while partial least squares regression and principal component regression modeling were performed in TQ Analyst. The coefficient of determination (R^2) and root mean square error (RMSE) between predicted and measured values were used to assess the predictive accuracy of the models.

Results and Discussion

Figure 1 illustrates three representative leaf spectral profiles with varying chlorophyll concentrations, randomly selected from 120 spectral datasets. Key spectral features (denoted A-M) exhibited a consistent reflectance pattern across all samples despite chlorophyll variations. The reflectance was lower in the blue light range (350~500nm), mainly because of carotenoid absorption in the leaves. The peaks D, J and N are mainly located at 910 nm, 1682 nm and 2238 nm, which are mainly caused by the three-order pan-frequency resonance of $C\text{-}H_3$ bonds, the frequency doubling absorption of lignin C=O and the deformation vibration of cellulose C-H. Valleys E, K, and M are located at 980 nm, 1788 nm, and 1916 nm, which are caused by the combined frequency mode of starch O-H expansion vibration and vacuolar water moleculevδ.

Figure 2 details a spectral preprocessing pipeline incorporating: (1) first/second derivatives and reciprocal logarithm transformations of reflectance data; (2) Savitzky-Golay 9-point smoothing for noise reduction. Beyond raw spectral analysis, these transformations identified chlorophyll-sensitive spectral regions. The first derivative enhances target reflectivity while suppressing linear backgrounds, the second derivative mitigates quadratic noise and high-frequency interference for improved soil factor quantification, and the logarithmic transform amplifies visible-band discrimination while reducing illumination-related multiplicative effects.

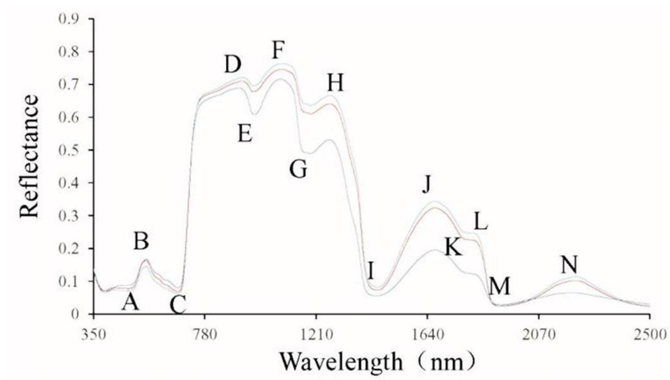

Fig.1. Spectral profiles across chlorophyll gradients.

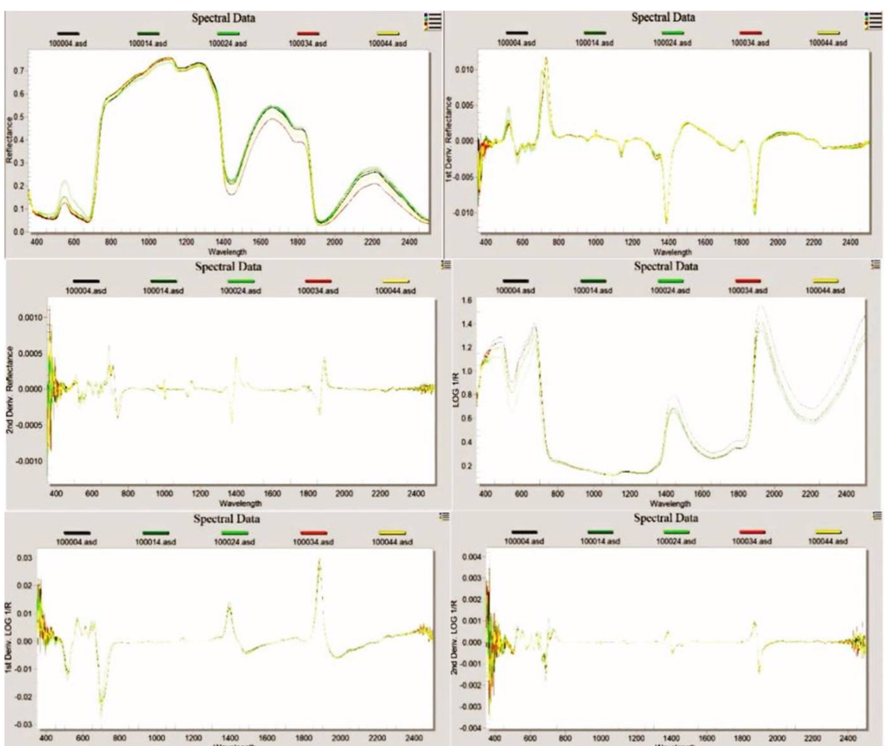

Fig.2. Comparative analysis of spectral features with different spectral pretreatments.

After applying first derivative, second derivative, and inverse logarithmic transformation to the reflectance spectral data, all processed data were smoothed using the Savitzky-Golay 9-point smoothing method. Partial Least Squares Regression was then employed to develop corresponding chlorophyll estimation models. The models were evaluated using the coefficient of determination and root mean square error. Specifically, a higher coefficient of determination and a lower root mean square error in the modeling phase indicate better model stability, while a higher coefficient of determination and a lower root mean square error in the prediction phase reflect stronger predictive capability. To prevent model overfitting, it is essential to minimize the dimensionality of the independent variables.

Following different preprocessing methods applied to the spectral data, both Partial Least Squares Regression was used to establish chlorophyll prediction models. The reliability of these models was assessed using the coefficient of determination, root mean square error, and standard error. Generally, a smaller root mean square error in prediction indicates better model performance. Furthermore, to avoid overfitting, the dimensionality of the independent variables should be kept as low as possible while maintaining model interpretability.

Fig. 3. The estimation models were established by PLSR for different spectral indexes. By comparing the established regression models, it can be concluded that the regression model established after preprocessing and differential transformation has better modeling accuracy and prediction accuracy than the model based on the original data. In the PLSR model, the model established by multiplicative scatter correction (MSC) processing of the smoothed spectrum and the second-order differential transformation had the best effect, Rc^2=0.9799, RMSEC=3.3027, SEC=3.3225, the NOR processing of the reflectance spectrum, and the second-order differential of the reciprocal logarithm had the best effect, Rc^2=0.9753, RMSEC=3.6629, SEC=3.6849, and SNV treatment of the reflectance spectrum. The model established by second-order differential of reciprocal logarithm has the best effect, with Rc^2=0.9720, RMSEC=3.9013, and SEC=3.9247.

Fig. 3 demonstrates PLSR-based comparative modeling of spectral preprocessing techniques, revealing enhanced predictive performance through differential transformations. MSC-processed smoothed spectra with second-derivative transformation achieved peak accuracy (Rc^2=0.9799, RMSEC=3.3027, SEC=3.3225). NOR-processed reflectance with log(1/R) second-derivative (Rc^2=0.9753, RMSEC=3.6629, SEC=3.6849). SNV-treated reflectance with log(1/R) second-derivative (Rc^2=0.9720, RMSEC=3.9013, SEC=3.9247). All transformed models outperformed raw spectral data in both calibration and validation accuracy.

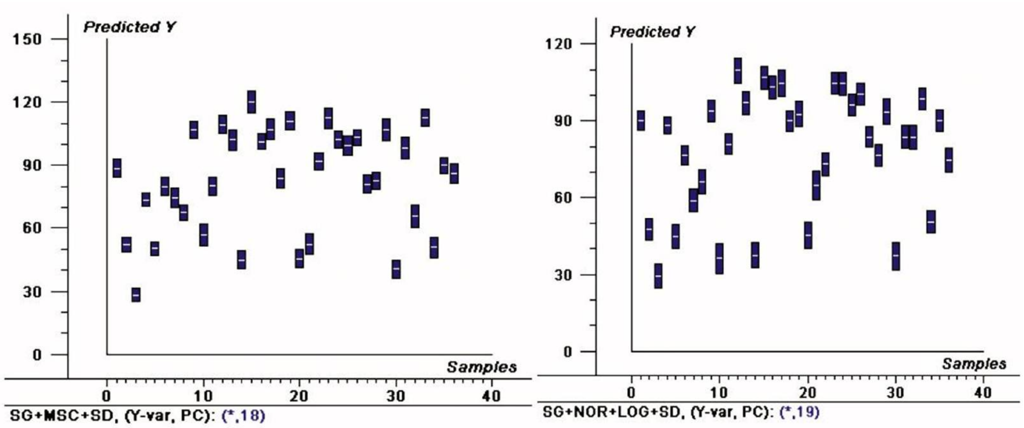

Fig. 3. Comparison of measured and predicted values based on partial least squares regression model.

This research establishes a quantitative PLSR model for monitoring jointing-stage maize canopy chlorophyll content using visible-near-infrared spectroscopy. Key methodological advancements include MSC, NOR, SNV preprocessing coupled with derivative transformations enhanced feature extraction. Second-derivative PLSR achieved peak performance (Rc^2=0.9799, RMSEC=3.3027, SEC=3.3225). Robust validation through cross-validation across diverse pedogenic materials confirmed model transferability. The framework enables rapid in-field chlorophyll estimation and provides actionable protocols for UAV-based spectral monitoring systems. Furthermore, this study collected sample data from the same region and performed cross-type validation of the constructed model, thereby further enhancing its generalization capability and reliability. The model offers a feasible approach for rapidly estimating rapeseed chlorophyll content within the study area and provides methodological guidance for chlorophyll monitoring in crop canopies using unmanned aerial vehicles and aerial remote sensing platforms. The experimental results confirm the viability of retrieving rapeseed canopy chlorophyll content using full-range hyperspectral data. However, the applicability of this technique across different ecological regions, crop species, and growth stages requires further investigation.

Acknowledgement

This study received funding from General Project of Humanities and Social Sciences Research for Henan Provincial Universities (2025-ZDJH-362).

References

Berger K, Atzberger C, Danner M, D'Urso G, Mauser W, Vuolo F and Hank T 2018. Evaluation of the PROSAIL model capabilities for future hyperspectral model environments: A review study. Remote Sens. **10**(1): 85.

Berger K, Verrelst J, Féret JB, Wang Z, Wocher M, Strathmann M, and Hank T 2021. Crop nitrogen monitoring: Recent progress and principal developments in the context of imaging spectroscopy missions. Remote Sens. Environ. **265**: 112671.

Camps-Valls G and Bruzzone L 2006. Kernel-based methods for hyperspectral image classification. IEEE Trans. Geosci. Remote Sens. **43**(6): 1351-1362.

Camps-Valls G, Verrelst J, Munoz-Mari J, Laparra V, Mateo-Jimenez F and Gomez-Dans J 2011. A survey on Gaussian processes for earth-observation data analysis: A comprehensive investigation. IEEE Geosci. Remote Sens. Mag. **4**(2): 58-78.

Cedric JS, Thomas R and Chris GC 2016. Near-infrared spectroscopy as a novel non-invasive tool to assess spiny lobster nutritional condition. PLoS One, **11**(7): e0159671.

Chen L and Li H 2024. Spectral transformer for chlorophyll-sensitive sub-band identification in crop phenotyping. ISPRS J. Photogramm. Remote Sens. **212**: 45-58.

Clark A, Mccord W and Zhang ZL 2022. Air resonance enhanced multiphoton ionization tagging velocimetry. Appl. Opt. **13**: 61.

Croft H, Arabian J, Chen JM, Shang JL and Liu JG 2020. Mapping within-field leaf chlorophyll content in agricultural crops for nitrogen management using landsat-8 imagery. Precis. Agric. **21**(4): 856-880.

Dong JY, Cheng XF, Fu TR, Ding JL and Fan XL 2008. Determination of chlorophyll a and b using absorption spectrum. Spectrosc. Spectral Anal. **28**(1): 141-144.

Dorigo WA, Zurita-Milla R, de Wit AJW, Brazile J, Singh R and Schaepman ME 2007. A review on reflective remote sensing and data assimilation techniques for enhanced agroecosystem modeling. Int. J. Appl. Earth Obs. Geoinf. **9**(2): 165-193.

Filella I and Peñuelas J 1994. The red edge position and shape as indicators of plant chlorophyll content, biomass and hydric status. Int. J. Remote Sens. **15**(7): 1459-1470.

Houborg R, McCabe MF, Cescatti A, Gao F, Schull M and Gitelson AA 2015. Joint leaf chlorophyll content and leaf area index retrieval from Landsat data using a regularized model inversion system (REGFLEC). Remote Sens. Environ. **159**: 203-221.

Jacquemoud S, Verhoef W, Baret F, Bacour C, Zarco-Tejada, PJ, Asner, GP and Ustin, SL 2009. PROSPECT+SAIL models: A review of use for vegetation characterization. Remote Sens. Environ. **113**: S56-S66.

Kim KY, Haagenson R, Kansara P, Rajaram H and Lakshmi V 2024. Augmenting daily MODIS LST with AIRS surface temperature retrievals to estimate ground temperature and permafrost extent in high mountain Asia. Remote Sens. Environ. **305**: 114075.

Kokaly RF and Clark RN 1999. Spectroscopic determination of leaf biochemistry using band-depth analysis of absorption features and stepwise multiple linear regression. Remote Sens. Environ. **67**(3): 267-287.

Li J, Wang Y and Zhang C 2023. Advancements and challenges in plant biochemical parameter estimation: A review. ISPRS J. Photogramm. Remote Sens. **195**: 1-15.

Li YS, Yao YK, Hao ZX, Zhou Y, Zhang WF, Zhu SW, Song YH and Shen CX 2024. Study on the diagnosis of rice nitrogen nutrition in Chongming District Shanghai based on leaf color information of different sensors. J. China Agric. Univ. **29**(12): 12-22.

Miller JR, Hare EW and Wu J 1990. Quantitative characterization of the vegetation red edge reflectance: I. An inverted-Gaussian model. Int. J. Remote Sens. **11**(10): 1755-1773.

Porcar-Castell A, Tyystjärvi E, Atherton J, van der Tol C, Flexas J, Pfündel EE and Berry JA 2014. Linking chlorophyll a fluorescence to photosynthesis for remote sensing applications: mechanisms and challenges. J. Exp. Bot. **65**(15): 4065-4095.

Silva MM, Santos JB, Santos EA, Santos MV, Sardinha LT and Ribeiro VHV 2018. Intoxication and physiological aspects of forage plants and weeds submitted to clomazone atmospheric waste. Planta Daninha, **36**: e018165080.

Sun Y, Wang D, Wang J, Zhang X and Liu S 2015. Non-destructive detection of chlorophyll content in maize canopy based on multispectral imaging. Trans. Chin. Soc. Agric. Eng. **31**(15): 173-179.

Ustin SL, Gitelson AA, Jacquemoud S, Schaepman M, Asner GP, Gamon JA and Zarco-Tejada P 2009. Retrieval of foliar information about plant pigment systems from high resolution spectroscopy. Remote Sens. Environ. 113: S67-S77.

Verrelst J, Camps-Valls G, Muñoz-Marí J, Rivera JP, Veroustraete F, Clevers JG and Moreno J 2015. Optical remote sensing and the retrieval of terrestrial vegetation bio-geophysical properties–A review. ISPRS J. Photogramm. Remote Sens. **108**: 273-290.

Verrelst J, Alonso L, Caicedo JPR, Moreno J and Camps-Valls G 2013. Gaussian process retrieval of chlorophyll content from imaging spectroscopy data. IEEE J. Sel. Top. Appl. Earth Obs. Remote Sens. **6**(2): 867-874.

Wang L and Bai YL 2005. Correlation between corn leaf spectral reflectance and leaf total nitrogen and chlorophyll content under different nitrogen level. Sci. Agric. Sin. **38**(11): 2268-2276.

Wang X, Li S, Zhang Y and Chen J 2023. Hyperspectral inversion of chlorophyll and water content in maize leaves under drought stress based on feature wavelength selection. Comput. Electron. Agric. **204**: 107541.

Wold S, Sjöström M and Eriksson L 2001. PLS-regression: a basic tool of chemometrics. Chemom. Intell. Lab. Syst. **58**(2), 109-130.

Yao X, Yang K, Zhao K, Lin Y and Zhang, J 2021. Estimating leaf chlorophyll content by integrating spectral and spatial features from UAV-based hyperspectral imagery. IEEE J. Sel. Top. Appl. Earth Obs. Remote Sens. **14**: 10249-10262.

Zhai Y and Li X 2014. Rapid detection of chlorophyll content in maize seedling leaves using near-infrared spectroscopy. Spectrosc. Spectral Anal. **34**(8) 2112-2116.

(Manuscript received on 20 May 2025; revised on 05 October 2025)